CrossMark

Anticorrosive Formulation Based of the Epoxy Resin–Polyaminoamide Containing Zinc Phosphate Inhibitive Pigment Applied on Sulfo-Tartaric Anodized AA 7075-T6 in NaCl Medium

O. Dagdag[1] · L. El Gana[2] · O. Hamed[3] · S. Jodeh[3] · A. El Harfi[1]

Abstract

The addition of zinc phosphate pigment to standard epoxy coatings has been investigated as an anticorrosive and eco-friendly additive. In this study, we prepared two epoxy coatings without and with zinc phosphate for corrosion protection of AA7075-T6 substrates for different time exposures in NaCl solution. The two epoxy coatings were evaluated by electrochemical impedance spectroscopy and their surfaces were characterized by scanning electron microscopy. The results show that the addition of zinc phosphate to the anticorrosive formulation (epoxy resin–polyaminoamide) facilitated the formation of a barrier film, enhanced the barrier anticorrosive properties of the coatings and therefore inhibited the penetration of aggressive corrosive ions to the AA7075-T6 surface.

Keywords Standard epoxy coating · Zinc phosphate · AA 7075-T6 · NaCl solution

1 Introduction

Aluminium alloys are widely used in the aerospace industry due to their light weight and high specific strength. However, these alloys are particularity sensitive to localized corrosion in chloride environments and need to be protected by a robust system [1–3]. For this purpose, organic coatings are usually applied to protect the aluminum substrates against corrosion. Up to now, epoxy-based organic coatings are the most used polymers [4, 5]. Anodizing is also applied to protect these aluminum substrates in aircraft structures.

Chromic anodizing (hexavalent chromium compounds) has mainly been utilized as an excellent corrosion protection [4].

However, because of environmental and health-related issues, several countries and the European Union are trying to ban the use of such kinds of treatment [6]. Other acid electrolyte baths have been developed and applied, such as sulfo-tartaric acid [7, 8]. Weak tartaric acid is added to strong sulfuric acid, a combination (a sulfo-tartaric bath) that limits the oxide dissolution and offers excellent corrosion resistance [9]. Organic coatings have been widely applied as a barrier layer on metal substrates to protect them against corrosion [10]. However, the organic coating deteriorate in the long term, resulting in a decline in the barrier performance. The durability and lifetime of an organic coating depends on several factors, such as the density of the coating cross-links, the coating chemistry and adhesion to the metal surface. Among various organic coatings, epoxy-based organic coatings have excellent corrosion resistance, excellent chemical resistance, a high cross-linking density and high adhesion to metal surfaces. However, penetration of aggressive corrosive ions into the standard epoxy coating from defects and micro-pores and diffusion of these corrosive agents to the metal/coating matrix interface results in the initiation of the corrosion process and deteriorates the coating matrix [11]. Inhibitive pigments, such as chromate-based pigments, are the commonest additions to anticorrosive formulations.

✉ O. Dagdag
   omar.dagdag@uit.ac.ma

✉ S. Jodeh
   sjodeh@hotmail.com

1   Laboratory of Agroresources, Polymers and Process Engineering (LAPPE), Department of Chemistry, Faculty of Science, Ibn Tofail University, BP 133, 14000 Kenitra, Morocco

2   Laboratory of Optoelectronics, Physical Chemistry of Materials and Environment, Department of Physics, Faculty of Science, Ibn Tofail University, BP 133, 14000 Kenitra, Morocco

3   Department of Chemistry, An-Najah National University, P. O. Box 7, Nablus, Palestine
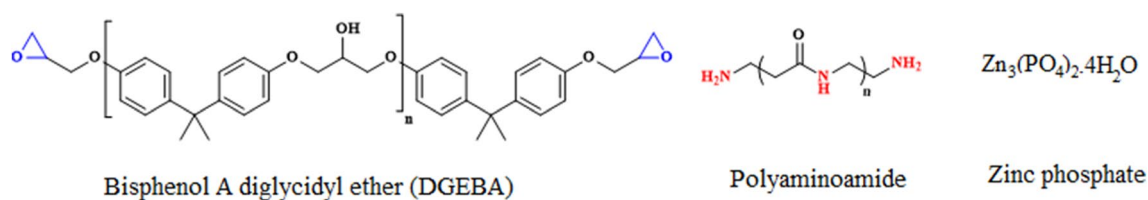
Fig. 1 Names and chemical structures used in the preparation of the coating materials

Table 1 Elementary chemical composition in weight percent of used of AA7075-d6

Element	Zn	Mg	Cu	Cr	Mn	Si	Fe	Al
Al 7075-T6	5.41	2.34	1.27	0.21	<0.01	0.07	0.12	Balance

However, because of the environmental rules, the use of this invaluable pigment in these anticorrosive formulations has been limited. Therefore, more solutions are being developed to find other alternative inhibitive pigments [12–14].

In recent decades, several less-toxic anticorrosive pigments have been used, for instance, zinc phosphate. This inhibitive pigment dissolves in water followed by precipitation of a barrier film on the substrate surface [15, 16]. This barrier film can block the active sites on the substrate surface and reduce the anodic dissolution process [17].

In this work, we have evaluated two epoxy coatings with and without zinc phosphate applied to protect AA7075-d6 substrates against corrosion were tested in an aggressive marine environment (3 wt% NaCl solution). The anticorrosive properties of the two epoxy coatings were monitored by electrochemical impedance spectroscopy (EIS) and the results were also confirmed by scanning electron microscopy (SEM).

2 Experimental

2.1 Materials and Methods

The epoxy resin bisphenol A diglycidyl ether (DGEBA) and hardener (polyaminoamide) used for the work were from MAPAERO-aerospace coatings. The pigment anticorrosive additive used in this work was zinc phosphate,y purchased from Aldrich. Figure 1 shows the names and chemical structures used in the preparation of the coating materials.

2.2 Preparation of AA7075 Substrates

The substrates used were 8.5 cm × 6.3 cm × 0.59 cm of AA7075-T6 and the chemical composition is shown in Table 1.

The aluminum samples were degreased with methyl ethyl ketone, air-dried, and dipped in a commercial

Table 2 Parameters of the sulfo-tartaric anodization

Parameters	Values for sulfo-tartaric anodization
Composition of the bath	36–44 g/L of sulfuric acid (H_2SO_4) 77–88 g/L of tartaric acid ($C_4H_6O_6$) Deionized water conductivity < 20 µS/cm
Electrical parameters	Voltage 0–14 V at a rate of 2.8 V/min Current density 0.5–1 A/dm^2
Bath temperature	36–39 °C
Duration of treatment	20–30 min

chrome-free alkaline cleaner (Turco) at 58 °C for 15 min. Then, they were dipped in a chrome-free commercial acid etching bath at 40 °C for 30 min. After each treatment step, the specimens were rinsed with distilled water.

The anodizing process of the samples of AA7075-d6 was carried in an industrial pilot plant containing a sulfo-tartaric bath. The sulfo-tartaric anodization was practiced with the parameters shown in Table 2.

2.3 Epoxy Resin Formulation and Aluminum Coating

Two epoxy formulations were prepared based on the epoxy resin (DGEBA) and mixed with a polyaminoamide curing agent (epoxy resin–polyaminoamide). A zinc phosphate (ZP) inhibitive pigment was added to the anticorrosive formulation to enhance the anticorrosive performance of the standard epoxy coating.

Two sets of Al-alloy samples were prepared, one coated with a standard DGEBA–polyaminoamide and the other one with DGEBA–polyaminoamide–ZP. The coatings were carried out using a film applicator. The coated samples were left at room temperature for 24 h before post-curing at 60 °C for 1 h. The thickness of the dried films was about 23 ± 2 µm.

2.4 Curing of DGEBA–Polyaminoamide

During the curing process, the epoxy resin and the curing agent polyaminoamide react to form a 3D thermoset polymer with multi-coordination sites of the hydroxyl and amino groups. A representative scheme of the possible reaction mechanism which occurs during the curing process is presented in Fig. 2 in which it is shown that, during the initiation stage of the curing process, the amine undergoes a nucleophilic addition at the epoxy ring [4, 5]. In the propagation stage, a high molecular weight crosslinked polymer forms.

2.5 Characterization

2.5.1 EIS Measurements

EIS evaluations were carried in a 3 wt% NaCl solution at 25 °C using Potentiostat PS 200. A three-electrode cell system was used for the electrochemical measurements consisting of a working electrode was AA7075-d6, a counter electrode was the Pt and the reference electrode was a saturated calomel electrode. The EIS measurements were carried out at an open-circuit potential (OCP), in the frequency range from 100 kHz to 0.01 Hz, with an AC amplitude of 10 mV

at OCP. The EIS results were analyzed using the EC-Lab V10.32 software fitting procedure.

The anticorrosion performance of the coated substrates was evaluated in an accelerated environment using a salt spray chamber. The corrosive nature was measured by the salt spray test according to the ASTM B117 standard.

2.5.2 Surface Characterization of Coating

The surface morphologies of the coatings were characterized by SEM (S3000H, Hitachi) operated at 20 keV.

3 Results and Discussion

3.1 EIS Measurements

Impedance diagrams are a valuable tool to obtain information about anticorrosion performance [18–21]. The Bode and Nyquist plots of the coatings obtained after different periods of exposure (1464, 2928 and 4392 h) and immersed in a 3 wt% NaCl solution for 2 h are shown in Figs. 3 and 4.

At the beginning of exposure during the 2 h of immersion in 3 wt% NaCl, the Bode plots for the two epoxy coatings characterized by the impedance modulus at low
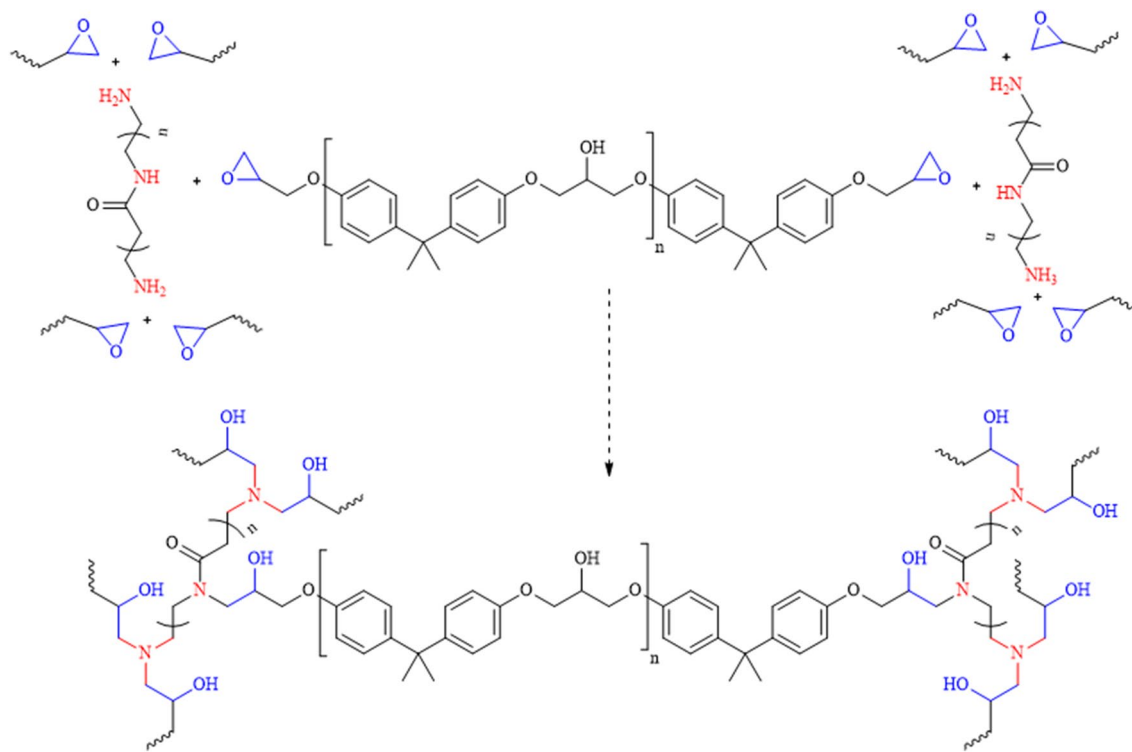

Fig. 2 The curing reaction mechanism of the DGEBA–polyaminoamide

frequencies ($|Z|_{0.01\ Hz}$) were high and greater than $10^5\ \Omega$ cm^2. The impedance modulus plot $|Z|_{0.01\ Hz}$ values of the standard epoxy coating begins from 545.95 kΩ cm^2 after 2 h immersion and finally reaches 241.90 kΩ cm^2 after 4392 h immersion. The decrease of impedance values with immersion time clearly denotes that the electrolyte disperses into the polymer matrix and reduces the barrier properties of the film. We have observed that the impedance modulus $|Z|_{0.01\ Hz}$ of the epoxy coating containing 5 wt% of ZP has a higher resistance starting from 1355.84 kΩ cm^2 after 2 h immersion and finally reaching 392.732 kΩ cm^2 after 4392 h immersion.

This may indicate that the epoxy coating containing ZP showed greater anticorrosive protection behavior because the inhibitive pigments can fill the micro-pores and defects present in the organic matrix by diminishing its porosity [22–24]. The EIS data are fitted using the electrical equivalent circuit shown in Fig. 5, where R_s, R_{pore}, R_{ct}, C_{coat} and C_{dl}

represent the solution resistance, coating resistance, charge transfer resistance and double layer capacitance, respectively. The electrochemical circuit was utilized in order to obtain R_s, R_{pore}, R_{ct}, C_{coat} and C_{dl} values from the Nyquist plots. To obtain a better fitting, a constant phase element (CPE) was used. The impedance of CPE is calculated using Eq. 1:

$$Z_{CPE} = \frac{1}{\left[f_0 (j \times w)^n \right]} \tag{1}$$

where f_0 is a proportionality coefficient, w is the angular frequency, and j is the imaginary number. The effective capacitance (Q) is calculated via the CPE parameters by [25]:

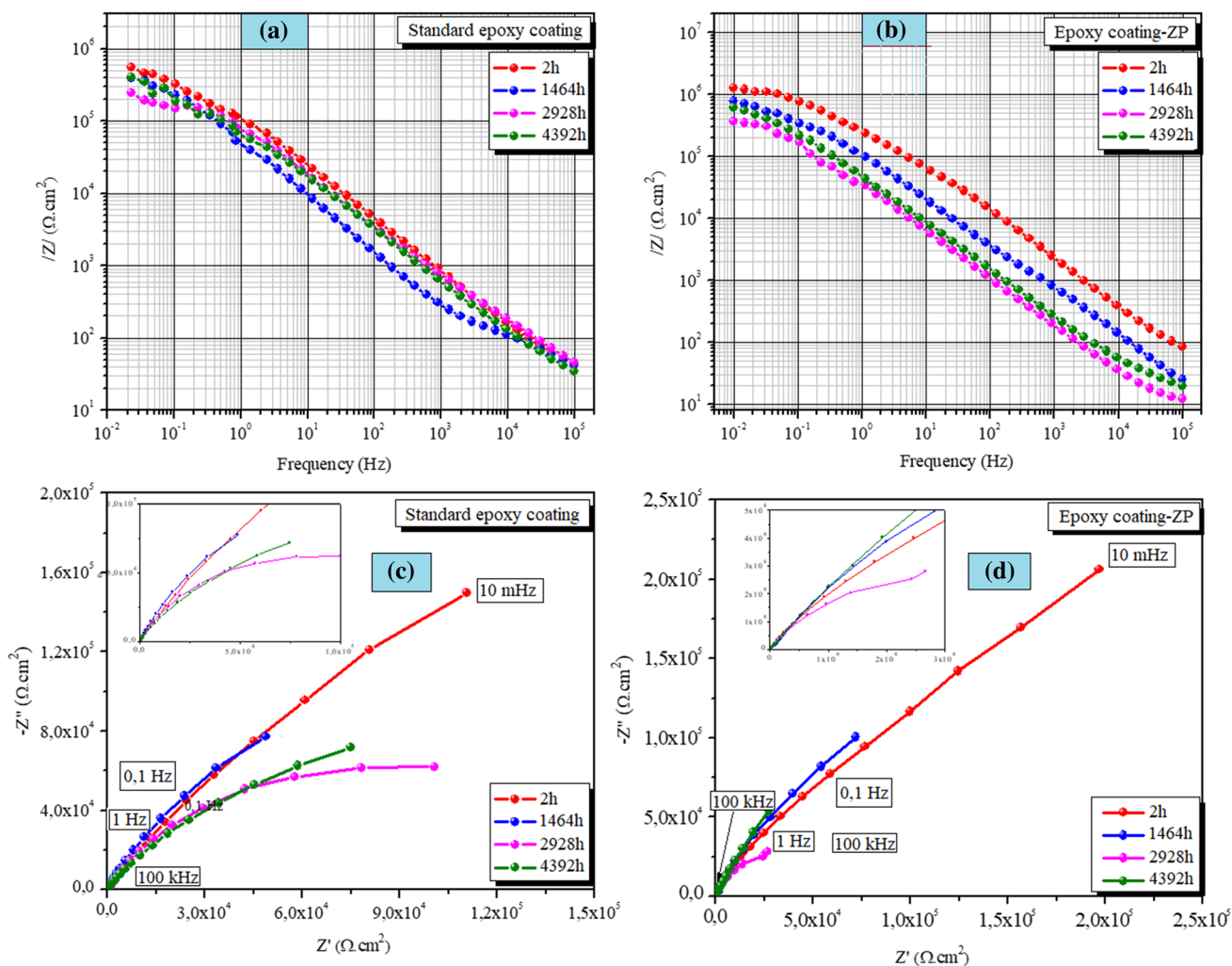$$Q = \frac{(Y_0 \times R)^{\frac{1}{n}}}{R} \tag{2}$$

Fig. 3 Bode and Nyquist plots obtained for the two epoxy coatings applied on AA7075-T6 samples for different periods of exposure (1464, 2928 and 4392 h) in the salt spray test chamber and immersiond in 3 wt% NaCl solution for 2 h
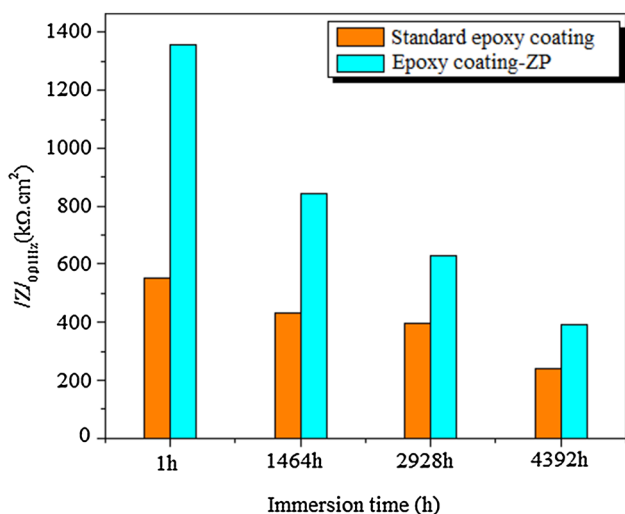
Fig. 4 The impedance modulus at low frequency ($|Z|_{0.01\ Hz}$) as a function of immersion time
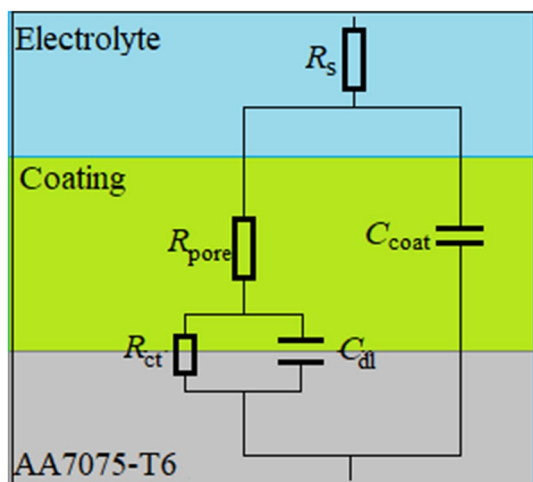

Fig. 5 The equivalent electrical circuit used to fit the measured impedance data

where Y_0 and n are the CPE admittance and CPE exponent, respectively. The anticorrosive protection of the coatings, the coating resistance (R_{pore}) and the charge transfer resistance (R_{ct}) were evaluated from the impedance diagrams.

The results summarized in Table 3 show that the R_{pore} and R_{ct} values of the epoxy coating-ZP increase significantly, an indication of the superiority of the epoxy coating-ZP over the standard epoxy coating.

Meanwhile, the higher values of R_{pore} and R_{ct} for the epoxy coating-ZP can be explained by the compatible and well-dispersed ZP in the coating matrix and the improving coating resistance against the transfer of corrosive agents (Cl^-, O_2 and H_2O) through the micro-pores and defects of the

coating matrix. The R_{pore} and R_{ct} values of the epoxy coatings decrease with immersion time, which is attributed to the diffusion of the corrosive agents into the coating matrix and access at the coating/metal interface.

Therefore, the corrosion reactions including anodic dissolution of the aluminum substrate and reduction of corrosive species (oxygen reduction) take place at the coating/metal interface, leading to delamination of the matrix.

Further, the C_{dl} which is related to the distribution of the ionic charge at the metal/coating interface [26] is lower for the epoxy coating-ZP for different times of immersion. The C_{dl} of the epoxy coating-ZP is lower than the standard epoxy coating. The C_{dl} value increases by increasing the immersion time due to the expansion of the active zones [27] and the fluctuations observed for the C_{dl} value during immersion is the result of the electrochemical process of the AA7075-d6 surface. Moreover, the C_{coat} for the epoxy coating-ZP sample is lower than for the standard epoxy coating after 2 h of immersion in NaCl solution, because the ZP inhibitive pigment fills the micro-pores and defects in the coating and decreases the water uptake into the coating matrix. The C_{coat} of the standard epoxy coating decreases to a stable value by extending the immersion time due to delamination of the coating matrix and filling the micro-pores and defects of the matrix with corrosion products [28]. However, the C_{coat} for the epoxy coating-ZP increases by increasing the immersion time to 1464 h, and then a decrease in the C_{coat} value is observed after immersion in the aggressive medium for 2928 h, which can be ascribed to the saturation of the ZP pigment. According to the results, the addition of ZP to the coating matrix effectively fills the micro-pores and defects. These mean that the ZP significantly enhances the anticorrosive properties and the barrier role of the coating matrix in the long term.

3.1.1 The Role of ZP in the Anticorrosion Process of the Coating Matrix

The ZP is an active pigment with anticorrosion behavior. The ZP can release solubilized ions including Zn^{2+} and PO_4^{3-} when exposed to the aggressive medium [29]. The dissociation of such an inhibitive pigment in the electrolyte is shown in Eq. (3).

$$Zn_3(PO_4)_2 \leftrightarrow 3Zn^{2+} + 2PO_4^{3-} \qquad (3)$$
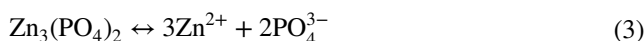
When the corrosive electrolyte reaches the metal surface, the following reactions (Eqs. (4, 5)) occur:

$$Al \rightarrow Al^{3+} + 3e^- \qquad (4)$$

$$2H_2O + O_2 + 4e^- \rightarrow 4OH^- \qquad (5)$$
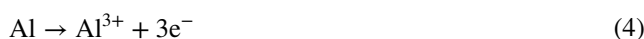
The dissolved agents of the pigments can reach the metal surface and react with OH^- anions and Al^{3+} cations

Table 3 Electrochemical data obtained from impedance plots of two epoxy coatings with and without zinc phosphate pigment applied to AA7075-T6 samples exposed to 3 wt% NaCl solution for 2 h at room temperature

Samples	Time (h)	$|Z|_{0.01\ Hz}$ ($k\Omega\ cm^2$)	C_{coat} ($\mu F/cm^2$)	R_{pore} ($k\Omega\ cm^2$)	C_{dl} ($\mu F/cm^2$)	R_{ct} ($k\Omega\ cm^2$)	χ^2
Standard epoxy coating	2	554.95	1.67	23.41	0.13	749.45	0.68
	1464	433.70	2.15	15.10	0.79	415.13	0.08
	2928	395.77	2.34	02.00	2.23	091.28	0.16
	4392	241.90	3.34	01.22	2.81	091.37	0.18
Epoxy coating-ZP	2	1355.8	0.55	213.5	0.12	1470.0	0.40
	1464	843.43	2.01	15.65	0.97	418.51	0.21
	2928	628.79	3.29	07.34	1.16	069.70	0.05
	4392	392.73	0.57	03.37	2.14	093.38	0.05

produced at ZPcathodic and anodic regions of the metal surface. As a result, a passive layer including, i.e., $Zn(OH)_2$ and $Al(OH)_3$, can be formed on the metal surface [30] as in Eqs. (6, 7):

$$Zn^{2+} + 2OH^- \rightarrow Zn(OH)_2 \downarrow \tag{6}$$

$$Al^{3+} + 3OH^- \rightarrow Al(OH)_3 \downarrow \tag{7}$$

A schematic illustration of the ZP mechanism with passive layer formation at the interface between the substrates and corrosive environment after accelerated corrosion assays is shown in Fig. 6.

3.2 Salt Spray Test

The digital images of the prepared epoxy coatings after 4392 h exposure are depicted in Fig. 7.

The standard epoxy coating shows corroded sites on the metal surface. For the epoxy coating-ZP, less degradation is observed as compared with the standard epoxy coating. Only small amounts of white rust appear inside the scratches.

Fig. 6 Schematic illustration of the zinc phosphate mechanism with passive layer formation at the interface between the substrates and corrosive environment after accelerated corrosion assays
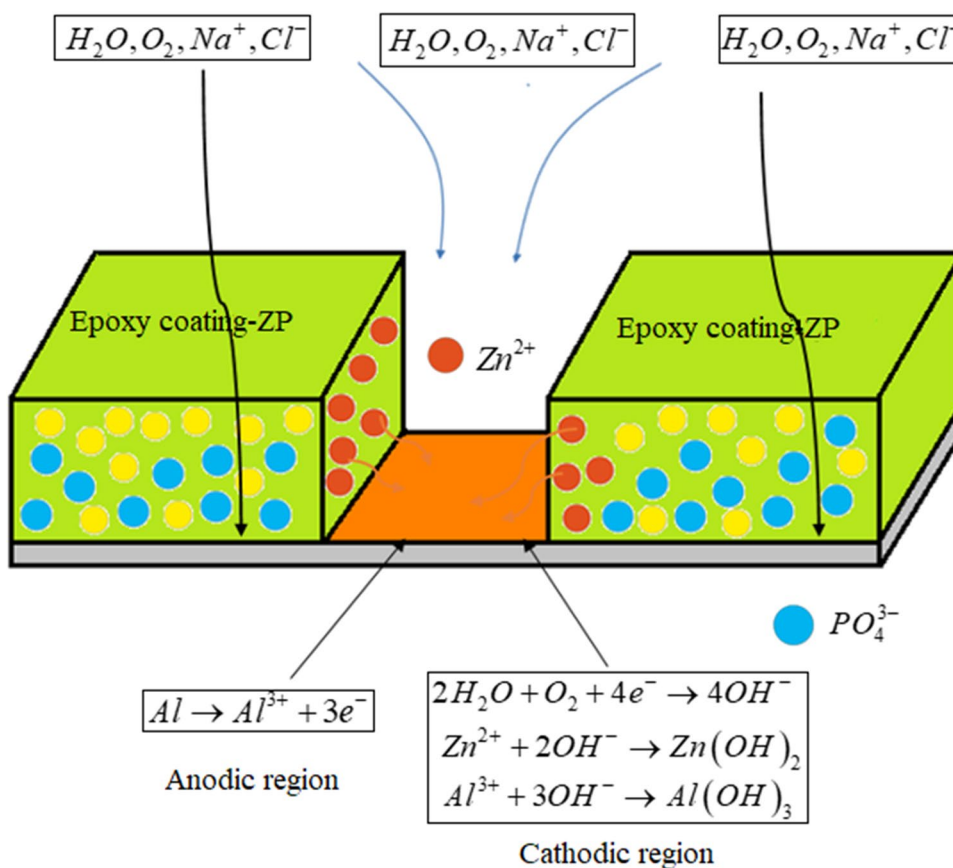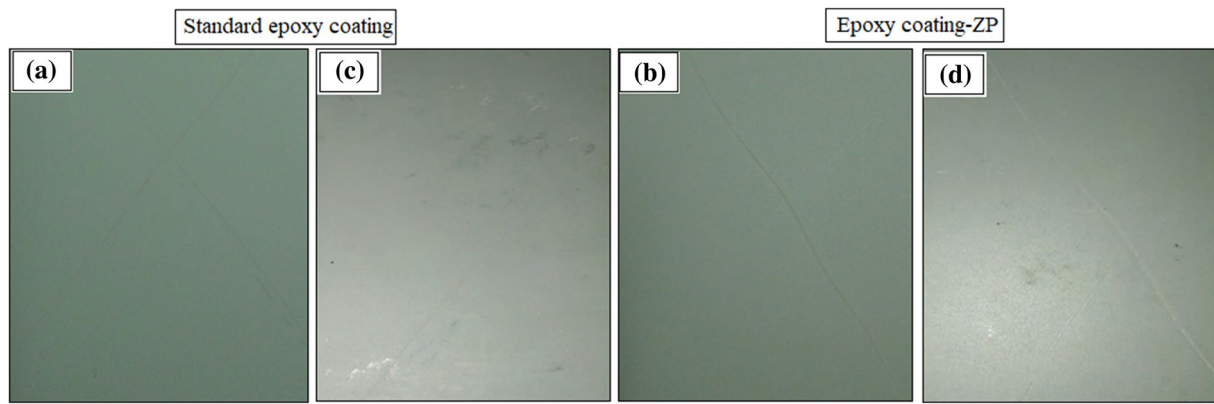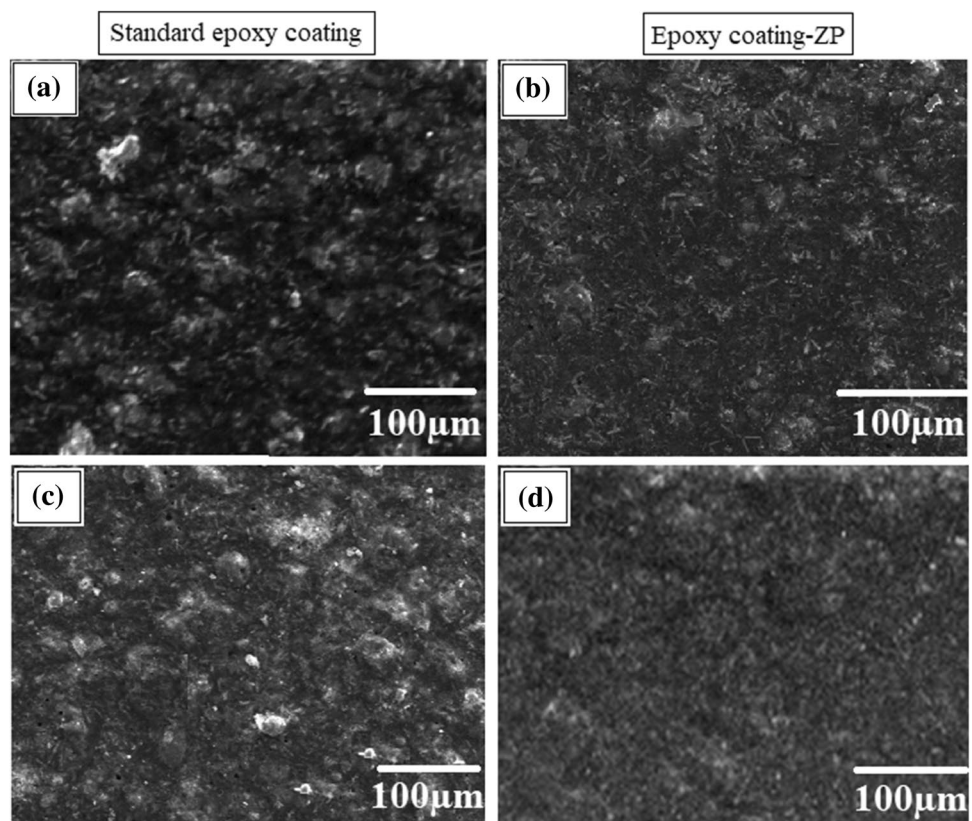
Fig. 7 Visual performance of the two epoxy coatings applied on the AA7075-T6 samples before and after 4392 h exposure in the salt spray test chamber

Fig. 8 SEM surface images of the two epoxy coatings applied on the AA7075-d6 samples before and after 4392 h exposure to the salt spray test chamber

3.3 Surface Morphological of Epoxy Coatings

Figure 8 shows SEM images of the surface of the two epoxy coatings with and without ZP before and after 4392 h exposure.

For the standard epoxy coating, as expected, the surface is uniform, smooth and free from defects, as shown in Fig. 8a.

For the epoxy coatings containing 5 wt% ZP, the presence of the ZP (Fig. 8b), well dispersed in the epoxy coating, is more uniform and homogeneous.

However, clear evidence of corrosion products and a porous morphology were observed on the standard epoxy coating surface after 4392 h exposure (Fig. 8c). Conversely, the surface morphology of the epoxy coating-ZP

showed fewer defects and very few corrosion products (Fig. 8d).

These results indicate that the addition of ZP facilitated the formation of a passive barrier film layer on the aluminium substrate and inhibited the diffusion of corrosive agents to the AA7075-T6 surface and enhanced the anticorrosive properties of the epoxy coating in the long term.

4 Conclusions

In this study, we have tested two formulations based on DGEBA epoxy resin and polyaminoamide (standard epoxy coating) and (epoxy coating-ZP) for the corrosion protection of AA7075-d6 substrates for different times of exposure (1464, 2928 and 4392 h). The obtained electrochemical approach shown by the EIS results and the surface morphology shown by SEM are in reasonable agreement, and they confirm that the ZP present in the coating matrix (epoxy coating-ZP) has a more effective anticorrosive performance than the standard epoxy coating. The Bode and Nyquist plots confirm the results obtained by the EIS. The ZP has outstanding barrier properties in epoxy coatings for preserving of AA7075-d6 in marine environments, so has great potential in marine corrosion protection, and is also environmentally friendly .

Compliance with Ethical Standards

Conflict of interest There are no conflicts to declare.

References

1. Li Y, Zhang P, Bai P, Wu L, Liu B, Zhao Z (2018) Microstructure and properties of Ti/TiBCN coating on 7075 aluminum alloy by laser cladding. Surf Coat Technol 334:142–149
2. Sabouri M, Khoei SM (2018) Plasma electrolytic oxidation in the presence of multiwall carbon nanotubes on aluminum substrate: morphological and corrosion studies. Surf Coat Technol 334:543–555
3. Aryanto D, Sudiro T (2018) Preparation of ferrosilicon-aluminium coating using a mechanical alloying technique: study of thermal annealing on their structural characteristics. Surf Coat Technol 337:35–43
4. Dagdag O, Hamed O, Erramli H, El Harfi A (2018) Anticorrosive performance approach combining an epoxy polyaminoamide–zinc phosphate coatings applied on sulfo-tartaric anodized aluminum alloy 5086. J Bio Tribo Corros. https://doi.org/10.1007/s40735-018-0168-6
5. Dagdag O, El Harfi A, El Gana L, Hlimi Z, Erramli H, Hamed O, Jodeh S (2019) The role of zinc phosphate pigment in the anticorrosion properties of bisphenol A diglycidyl ether-polyaminoamide coating for aluminum alloy AA2024-T3. J Bio Tribo Corros. https://doi.org/10.1007/s40735-018-0200-x
6. Harscoet E, Froelich D (2008) Use of LCA to evaluate the environmental benefits of substituting chromic acid anodizing (CAA). J Clean Prod 16(12):1294–1305
7. García-Rubio M, De Lara MP, Ocón P, Diekhoff S, Beneke M, Lavía A, García I (2009) Effect of postreatment on the corrosion behaviour of tartaric–sulphuric anodic films. Electrochim Acta 54(21):4789–4800
8. Sulka GD, Parkoła KG (2007) Temperature influence on well-ordered nanopore structures grown by anodization of aluminium in sulphuric acid. Electrochim Acta 52(5):1880–1888
9. Kuznetsov B, Serdechnova M, Tedim J, Starykevich M, Kallip S, Oliveira MP et al (2016) Sealing of tartaric sulfuric (TSA) anodized AA2024 with nanostructured LDH layers. RSC Adv 6(17):13942–13952
10. Renaud A, Poorteman M, Escobar J, Dumas L, Bonnaud L, Dubois P, Olivier MG (2017) A new corrosion protection approach for aeronautical applications combining a Phenol-paraPhenyleneDiAmine benzoxazine resin applied on sulfo-tartaric anodized aluminum. Prog Org Coat 112:278–287
11. Niroumandrad S, Rostami M, Ramezanzadeh B (2016) Effects of combined surface treatments of aluminium nanoparticle on its corrosion resistance before and after inclusion into an epoxy coating. Prog Org Coat 101:486–501
12. Hu T, Shi H, Fan S, Liu F, Han EH (2017) Cerium tartrate as a pigment in epoxy coatings for corrosion protection of AA 2024-T3. Prog Org Coat 105:123–131
13. Prosek T, Thierry D (2004) A model for the release of chromate from organic coatings. Prog Org Coat 49(3):209–217
14. Zhang W, Buchheit RG (2003) Effect of ambient aging on inhibition of oxygen reduction by chromate conversion coatings. Corrosion 59(4):356–362
15. Dagdag O, El Harfi A, Essamri A, El Bachiri A, Hajjaji N, Erramli H et al (2018) Anticorrosive performance of new epoxy-amine coatings based on zinc phosphate tetrahydrate as a nontoxic pigment for carbon steel in NaCl medium. Arab J Sci Eng. https://doi.org/10.1007/s13369-018-3160-z
16. Dagdag O, El Harfi A, Essamri A, El Gouri M, Chraibi S, Assouag M et al (2018) Phosphorous-based epoxy resin composition as an effective anticorrosive coating for steel. Int J Ind Chem 9(3):231–240
17. Blustein G, Deyá MC, Romagnoli R, Del Amo B (2005) Three generations of inorganic phosphates in solvent and water-borne paints: a synergism case. Appl Surf Sci 252(5):1386–1397
18. Snihirova D, Lamaka SV, Montemor MF (2012) "SMART" protective ability of water based epoxy coatings loaded with $CaCO_3$ microbeads impregnated with corrosion inhibitors applied on AA2024 substrates. Electrochim Acta 83:439–447
19. Echeverría M, Abreu CM, Echeverría CA (2014) Assessing pretreatment effect on the protective properties of different coating systems against marine corrosion. Corrosion 70(12):1203–1218
20. Mahmoodi A, Ebrahimi M (2018) Role of a hybrid dye-clay nanopigment (DCNP) on corrosion resistance of epoxy coatings. Prog Org Coat 114:223–232
21. Ding J, ur Rahman O, Peng W, Dou H, Yu H (2018) A novel hydroxyl epoxy phosphate monomer enhancing the anticorrosive performance of waterborne graphene/epoxy coatings. Appl Surf Sci 427:981–991
22. Deflorian F, Rossi S, Fedel M, Motte C (2010) Electrochemical investigation of high-performance silane sol–gel films containing clay nanoparticles. Prog Org Coat 69(2):158–166

23. Montemor MF, Snihirova DV, Taryba MG, Lamaka SV, Kartsonakis IA, Balaskas AC et al (2012) Evaluation of self-healing ability in protective coatings modified with combinations of layered double hydroxides and cerium molibdate nanocontainers filled with corrosion inhibitors. Electrochim Acta 60:31–40

24. Ammar S, Ramesh K, Vengadaesvaran B, Ramesh S, Arof AK (2016) Amelioration of anticorrosion and hydrophobic properties of epoxy/PDMS composite coatings containing nano ZnO particles. Prog Org Coat 92:54–65

25. Yu D, Wen S, Yang J, Wang J, Chen Y, Luo J, Wu Y (2017) RGO modified ZnAl-LDH as epoxy nanostructure filler: a novel synthetic approach to anticorrosive waterborne coating. Surf Coat Technol 326:207–215

26. Konios D, Stylianakis MM, Stratakis E, Kymakis E (2014) Dispersion behaviour of graphene oxide and reduced graphene oxide. J Colloid Interface Sci 430:108–112

27. Wu LK, Zhang JT, Hu JM, Zhang JQ (2012) Improved corrosion performance of electrophoretic coatings by silane addition. Corros Sci 56:58–66

28. Ghasemi-Kahrizsangi A, Shariatpanahi H, Neshati J, Akbarinezhad E (2015) Corrosion behavior of modified nano carbon black/epoxy coating in accelerated conditions. Appl Surf Sci 331:115–126

29. Mousavifard SM, Nouri PM, Attar MM, Ramezanzadeh B (2013) The effects of zinc aluminum phosphate (ZPA) and zinc aluminum polyphosphate (ZAPP) mixtures on corrosion inhibition performance of epoxy/polyamide coating. J Ind Eng Chem 19(3):1031–1039

30. Jalili M, Rostami M, Ramezanzadeh B (2015) An investigation of the electrochemical action of the epoxy zinc-rich coatings containing surface modified aluminum nanoparticle. Appl Surf Sci 328:95–108